



Cite this: *New J. Chem.*, 2021, 45, 2147

A recyclable cobalt(III)–ammonia complex catalyst for catalytic epoxidation of olefins with air as the oxidant†

Chenlong Wang,^a Hongju Zhan,^b Xinhuan Lu,^{*a} Run Jing,^a Haifu Zhang,^a Lu Yang,^a Xixi Li,^a Fanfan Yue,^a Dan Zhou^{id}^a and Qinghua Xia^{id}^{*a}

[Co(NH₃)₆]Cl₃ and other ammonia complexes with different external anions or metal ions were synthesized to catalyze the epoxidation of α -pinene. The synthesized complexes were characterized using XRD, SEM, TGA, FTIR and UV spectra. With air as the oxidant, [Co(NH₃)₆]Cl₃ exhibited excellent catalytic activity for the epoxidation of α -pinene among the prepared complexes. The conversion of α -pinene reached 97.4%, with 98.3% selectivity of epoxide when using a small amount of cumene hydroperoxide (CHP) as the initiator. The results revealed that a single Co(III) system can also catalyze the epoxidation process in the absence of Co(II), even showing better catalytic performance than single Co(II). Recycling experiments showed that there was no significant drop in activity after 10 cycles, demonstrating that it is a stable and efficient heterogeneous catalyst for the epoxidation of α -pinene. The excellent recycling performance may be attributed to the stability of the coordination complex itself.

Received 8th November 2020,
Accepted 31st December 2020

DOI: 10.1039/d0nj05466f

rsc.li/njc

1. Introduction

Epoxy compounds are usually produced by oxidation of olefins,¹ which are important synthetic intermediates² in organic reactions, and can be used to prepare epoxy resins, coatings,³ advanced building blocks, *etc.* Besides, alcohols, hydroxy ethers^{4,5} and some other chemicals which have wide applications need epoxides as the starting material for their synthesis. For example, α -pinene oxide, which in nature is formed by the epoxidization of α -pinene in some plants, is an important raw material used in the production of drugs.⁶ Thus, developing efficient and highly selective catalysts to catalyze the epoxidation of olefins is a research hotspot in the field of catalysis.⁷

Traditionally, the epoxidation of olefins in industrial production requires the addition of stoichiometric organic peroxides⁸ or peracids⁹ as oxidizing agents. However, using peracids as the oxidant will produce acidic toxic wastes,^{10,11} which are difficult to dispose, and organic peroxides such as *tert*-butyl hydroperoxide

(TBHP) are expensive and dangerous.¹² In contrast, abundant and readily available molecular oxygen, which is also environmentally friendly, is undoubtedly the most suitable oxidant. Previous studies on olefin epoxidation with molecular oxygen as an oxidant have been carried out.¹³ Our group has recently also made considerable progress in enhancing the reactivity of air with α -pinene by using microwaves.¹⁴

From an economic and feasibility point of view, it is more attractive to use cheap and readily available transition metals instead of Ag,¹⁵ Au¹⁶ or other noble metals as the catalyst for epoxidation reactions.^{3,17,18} Among the transition metals, Ti, Mo, W, V, and Re have been early and extensively researched.^{19–25} Recently, a series of catalysts based on Fe,²⁶ Co,^{27–29} Ni,³⁰ and Mn³¹ have also been studied and developed to catalyze the epoxidation reaction. Since the complexes of transition metal and Schiff base have been considered as one of the most efficient catalysts for epoxidation reaction,^{32–34} numerous studies on the complexes of different metals with the Schiff base have been carried out.^{35,36} However, metal complexes are applicable to homogeneous systems under normal conditions,^{37–39} resulting in difficulty in the separation of catalysts from the reaction system. Comparatively, heterogeneous catalytic systems can overcome this shortcoming, thus the transform of homogeneous catalysts to heterogeneous ones has always been a research direction for catalytic scholars. To this end, various supported metal complexes^{40,41} have been developed to catalyze the epoxidation process. The transition metal-containing

^a Hubei Collaborative Innovation Center for Advanced Organic Chemical Materials, Ministry-of-Education Key Laboratory for the Synthesis and Application of Organic Functional Molecules, Ministry-of-Education Key Laboratory for Green Preparation and Application of Functional Materials, Hubei University, Wuhan 430062, P. R. China. E-mail: xinhuan003@aliyun.com, xiaqh518@aliyun.com

^b Jingchu University of Technology, Jingmen 448000, P. R. China

† Electronic supplementary information (ESI) available. See DOI: 10.1039/d0nj05466f

MOF materials can be also directly modified⁴² to be heterogeneous catalysts. However, the uneven distribution and easy leaching of active sites lead to reduction in activity or even deactivation, which is not suitable for continuous industrial production.^{23,43}

Mascharak *et al.* have reported that olefin epoxidation is carried out by radicals and Co(III), which is an intermediate that promotes the reaction in the Co(II) catalytic system.⁴⁴ Possibly, Co(III) can facilitate to promote the formation of RO· radicals during the reaction. Herein, we synthesize Co(III)-based [Co(NH₃)₆]Cl₃ material as a heterogeneous catalyst, which can avoid the problem of the difficulty in separating of the catalyst from the product.⁴⁵ When introducing air as the oxidant, the as-prepared catalyst performed excellent catalytic activity on the epoxidation of α -pinene, giving 97.4% conversion and 98.3% selectivity of epoxide. The recycling performance of the catalyst is also tested, and the results show that the activity is still well maintained after 10 recycles, with no significant decrease in activity.

2. Experimental section

2.1. Materials

The main reagents including CoCl₂·6H₂O (AR, Aladdin), Co(NO₃)₂·6H₂O ($\geq 99\%$, Aladdin), Coconut shell charcoal (Hainan), NH₄Cl ($\geq 99.5\%$, Sinopharm), NH₃·H₂O (25–28%, Sinopharm), HCl (hydrochloric acid, 36–38%, Sinopharm), THF (tetrahydrofuran, $\geq 99.5\%$, Sinopharm), Ni(NO₃)₂·6H₂O ($\geq 99\%$, Sinopharm), CuSO₄·5H₂O ($\geq 99\%$, Sinopharm), ZnCl₂ ($\geq 99\%$, Kelong), CHP (Cumene hydroperoxide, $\geq 72\%$, Sinopharm), TBHP (*tert*-butyl hydroperoxide, $\geq 65\%$, Sinopharm), H₂O₂ ($\geq 30\%$, Sinopharm), α -pinene epoxide ($\geq 95\%$, TGI), DMF (*N,N*-dimethyl formamide, $\geq 98.5\%$, Sinopharm), DMA (*N,N*-dimethyl acetamide, $\geq 98.5\%$, Sinopharm), α -pinene ($\geq 98\%$, Macklin), β -pinene ($\geq 98\%$, Macklin), 1-dodecene ($\geq 95\%$, Macklin), cyclooctene ($\geq 95\%$, Macklin), α -methylstyrene ($\geq 99\%$, Macklin) and styrene ($\geq 99\%$, Sinopharm) were directly used without further purification.

2.2. Preparation of catalysts

2.2.1. Synthesis of [Co(NH₃)₆]Cl₃. [Co(NH₃)₆]Cl₃ was prepared using the method reported by Bjerrum and McReynold.⁴⁶ NH₄Cl (4.0 g) was dissolved in a beaker with deionized water (8.4 g) under stirring, then CoCl₂·6H₂O (6.0 g) and coconut shell charcoal (0.4 g) were mixed into the above solution. Subsequently, NH₃·H₂O (12.5 mL) was slowly added into the beaker in an ice bath and then the beaker was sealed with a plastic wrap until the temperature of the solution dropped to 0 °C. The solution was heated and kept at 60 °C for 30 min after 5% H₂O₂ (13.5 mL) was injected to the solution. After cooling the solution to 0 °C, black precipitate was obtained by filtration. Then, the precipitate was dissolved in 60 mL of boiled water containing concentrated HCl (1.7 mL) and filtered immediately. Concentrated HCl (6.7 mL) was slowly added to the above filtrate and the orange-yellow solid could be precipitated during cooling. Then, [Co(NH₃)₆]Cl₃ was collected by vacuum suction filtration.

The product was directly used as a catalyst after drying at 80 °C for 24 h.

2.2.2. Synthesis of [Co(NH₃)₅Cl]Cl₂. NH₄Cl (10.0 g) and CoCl₂·6H₂O (50.0 g) were dissolved using concentrated NH₃·H₂O (160 mL), then 30% H₂O₂ (40 mL) was added slowly into the above solution under stirring (foaming phenomenon was observed during this period). Purplish red precipitate was generated while adding HCl (16 mL) slowly. After cooling, the precipitate was filtered and washed with diluted hydrochloric acid and ethanol. Purplish red [Co(NH₃)₅Cl]Cl₂ was obtained after drying at 80 °C for 24 h.

2.2.3. Synthesis of [Co(NH₃)₆](NO₃)₃. The synthesis process of [Co(NH₃)₆](NO₃)₃ was similar to that of [Co(NH₃)₆]Cl₃, except that CoCl₂·6H₂O and NH₄Cl were replaced by equimolar amounts of Co(NO₃)₂·6H₂O and NH₄NO₃.

2.2.4. Synthesis of [Co(NH₃)₆](Ac)₃. The synthesis process of [Co(NH₃)₆](Ac)₃ was similar to that of [Co(NH₃)₆]Cl₃, except that HAc (Acetic acid) instead of concentrated HCl was added into the filtrate. [Co(NH₃)₆](Ac)₃ was obtained after cooling and filtering.

2.2.5. Synthesis of [Co(NH₃)₅Cl]SO₄. Concentrated H₂SO₄ and synthesized [Co(NH₃)₅Cl]Cl₂ were mixed in the ratio of 1 : 3. Subsequently, the solution was diluted with hot water (70 °C) until bubble (HCl) generation ceased. Then [Co(NH₃)₅Cl]SO₄·2H₂O could be obtained by cooling and filtering.

2.3. Characterization of the complex materials

X-ray diffraction (XRD) patterns of catalysts were collected using a Bruker D8A25 diffractometer with Cu K α as the radiation ($\lambda = 1.54184 \text{ \AA}$). The test conditions were a scanning range from $2\theta = 5$ to 80° , a speed of $10^\circ \text{ min}^{-1}$ and operated at 40 kV and 40 mA. Scanning electron microscope (SEM) images was taken using a JEOL JSM-6510 A to investigate the surface morphology and size of the catalyst. The IR spectra of samples in the range of 400–4000 cm^{-1} were recorded using a OPUS Fourier Transform Infrared Spectrophotometer. The UV-Vis spectra of materials were detected using a Shimadzu UV-2550 spectrometer with a scanning range from 800 to 200 cm^{-1} . X-ray photoelectron spectra (XPS) of the sample were recorded using a Thermo Fisher Scientific ESCALAB 250Xi spectrometer under 0.5 E_v of energy resolution. Additionally, thermogravimetric study (TGA) of the catalysts was conducted using a METTLER-TOLEDO TGA2 instrument, with N₂ at a flow rate of 40 mL min^{-1} as the shielding gas and testing from 30 to 1000 °C at a heating rate of $10^\circ \text{ C min}^{-1}$. The results of the NH₃ temperature-programmed desorption (NH₃-TPD) analysis of the material were recorded using an automatic gas sorption analyzer (TP-5076).

2.4. Epoxidation reactions of α -pinene

Typically, the reaction process comprised the following steps: 5 mg of catalyst, 10 g of DMF, 3 mmol of α -pinene and 0.3 mmol of CHP were added into a two-necked glass reactor. Then, the reactor was placed in a water bath at 90 °C with a cryogenic-liquid condenser. The flow rate of air was 40 mL min^{-1} . After reacting for 5 h under stirring, the product was separated by

centrifugation. Subsequently, the filtrate was collected and analyzed using a gas chromatography (GC) instrument that was equipped with a capillary column (Rtx-5, 30 m × 0.25 mm × 0.25 μm) and an FID detector, in which chlorobenzene was used as the internal standard to analyze different components.

3. Result and discussion

3.1. Structural descriptions

The XRD patterns of the synthesized $[\text{Co}(\text{NH}_3)_6]\text{Cl}_3$ are shown in Fig. 1. The diffraction peaks of the material were exactly consistent with the simulated peaks, showing obvious crystal peaks at $2\theta = 15.0^\circ, 15.5^\circ, 16.8^\circ, 17.8^\circ, 24.3^\circ, 24.9^\circ, 25.6^\circ, 34.0^\circ$ and 36.2° , which indicated that $[\text{Co}(\text{NH}_3)_6]\text{Cl}_3$ had been successfully synthesized. Fig. S1 (ESI[†]) compares the differences in the XRD patterns between $[\text{Co}(\text{NH}_3)_6]\text{Cl}_3$ and other synthesized cobalt compounds ($[\text{Co}(\text{NH}_3)_5\text{Cl}]\text{Cl}_2$ and $[\text{Co}(\text{NH}_3)_5\text{Cl}]\text{SO}_4$), in which the different characteristic diffraction peaks indicated that these synthesized catalysts exhibited an entirely different crystal structure. Moreover, it could be observed that the intensity of the diffraction peaks of $[\text{Co}(\text{NH}_3)_6]\text{Cl}_3$ was obviously higher than that of the $[\text{Co}(\text{NH}_3)_5]^{3+}$ complexes, which might endow it with considerable catalytic performance.

Fig. 2 shows the infrared spectra of the $[\text{Co}(\text{NH}_3)_6]\text{Cl}_3$ material. It could be seen from the figure that there are four main characteristic absorption peaks, including (1) the strong absorption peak at 820 cm^{-1} belonging to the Co–N rocking vibration, (2) the sharp absorption peak at 1320 cm^{-1} , which is assigned to the symmetrical bending vibration of the N–H bond, (3) the weak broad peak at 1580 cm^{-1} , which is attributed to N–H unsymmetrical bending vibration, and (4) the absorption peak at 3120 cm^{-1} corresponding to the symmetrical stretching vibration of the N–H bond. All of them are in agreement with

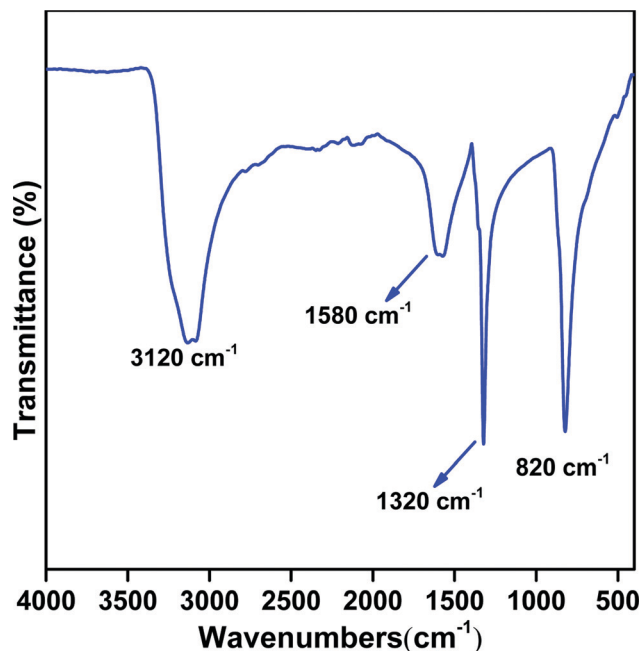


Fig. 2 The IR spectra of $[\text{Co}(\text{NH}_3)_6]\text{Cl}_3$.

those reported in the literature.^{47,48} The IR spectra of different cobalt–ammonia complexes are shown in Fig. S2 (ESI[†]). $[\text{Co}(\text{NH}_3)_5\text{Cl}]\text{Cl}_2$, $[\text{Co}(\text{NH}_3)_6](\text{Ac})_3$ and $[\text{Co}(\text{NH}_3)_6]\text{Cl}_3$ exhibited similar spectra, with characteristic absorption peaks appearing at about $820, 1320, 1580$ and 3120 cm^{-1} , consistent with those reported in the literature.⁴⁶ However, the IR spectra of $[\text{Co}(\text{NH}_3)_5\text{Cl}]\text{SO}_4$ and $[\text{Co}(\text{NH}_3)_6](\text{NO}_3)_3$ were obviously different from those of others. The absorption peaks at 610 and 1090 cm^{-1} in the spectra of $[\text{Co}(\text{NH}_3)_5\text{Cl}]\text{SO}_4$ were typical absorption of SO_4^{2-} . The absorption peaks at 1320 cm^{-1} of $[\text{Co}(\text{NH}_3)_6](\text{NO}_3)_3$ seemed wider and stronger than those of other complexes, which could be ascribed to the overlap interference between stretching vibration of NO_3^- and symmetrical bending vibration of the N–H bond.

Fig. 3 shows the results of SEM micro-morphology analysis of different cobalt–ammonia complexes. From the figure, it could be seen that all the complexes exhibited micron sized bulk morphology with an uneven grain size. $[\text{Co}(\text{NH}_3)_6]\text{Cl}_3$ (a and a') possessed a relatively smooth surface and displayed regular columnar morphology. Another complex with regular morphology was $[\text{Co}(\text{NH}_3)_5\text{Cl}]\text{Cl}_2$ (d and d'). However, the morphology of $[\text{Co}(\text{NH}_3)_6](\text{Ac})_3$ (b and b'), $[\text{Co}(\text{NH}_3)_6](\text{NO}_3)_3$ (c and c'), and $[\text{Co}(\text{NH}_3)_5\text{Cl}]\text{SO}_4$ (e and e') was amorphous and the three samples exhibited uneven sizes from a few microns to tens. Fig. S3 (ESI[†]) compares the UV-Vis spectra of the synthesized $[\text{Co}(\text{NH}_3)_5\text{Cl}]\text{Cl}_2$, $[\text{Co}(\text{NH}_3)_6](\text{Ac})_3$, $[\text{Co}(\text{NH}_3)_6]\text{Cl}_3$ and $[\text{Co}(\text{NH}_3)_6](\text{NO}_3)_3$. According to the literature,⁴⁹ the characteristic peaks at 340 and 470 nm were typical absorption peaks of a low spin octahedral coordination compound ($d^6[\text{Co}(\text{NH}_3)_6]^{3+}$), which belong to ${}^1\text{A}_{1g} \rightarrow \text{T}_{1g}$ and ${}^1\text{A}_{1g} \rightarrow \text{T}_{2g}$, respectively. But the absorption peaks of $[\text{Co}(\text{NH}_3)_5\text{Cl}]\text{Cl}_2$ were at 370 and 550 nm , ascribed to the different coordination environment of $\text{Co}(\text{III})$

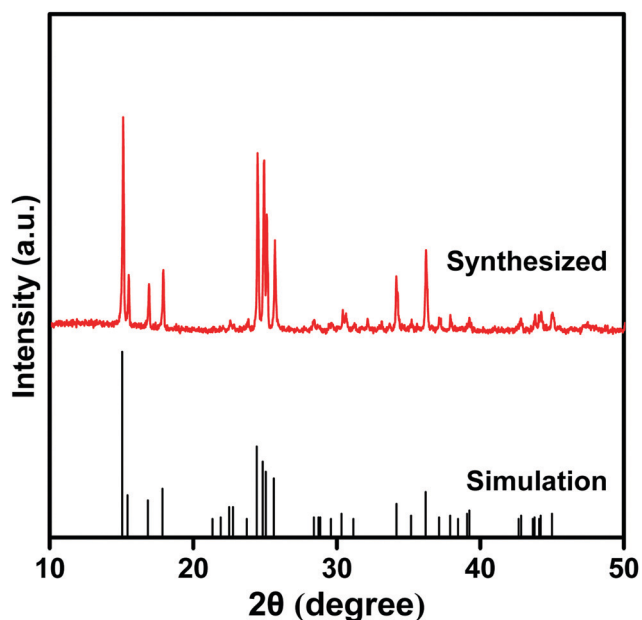


Fig. 1 The XRD patterns of $[\text{Co}(\text{NH}_3)_6]\text{Cl}_3$ synthesized and the simulated one.

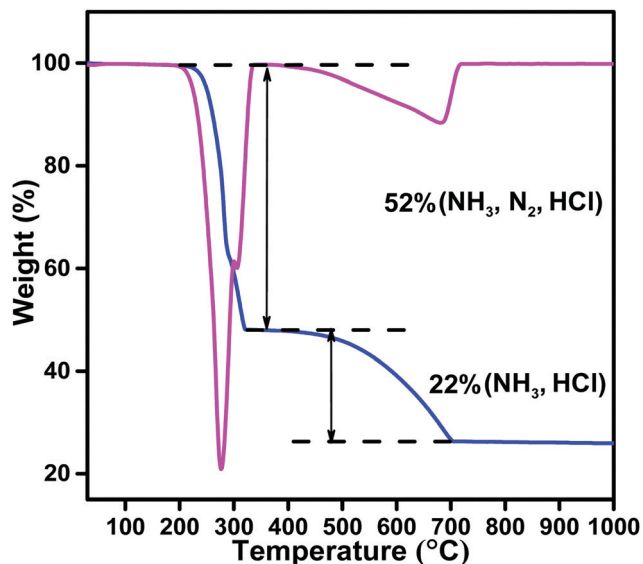


Fig. 4 TG curves of $[\text{Co}(\text{NH}_3)_6]\text{Cl}_3$.

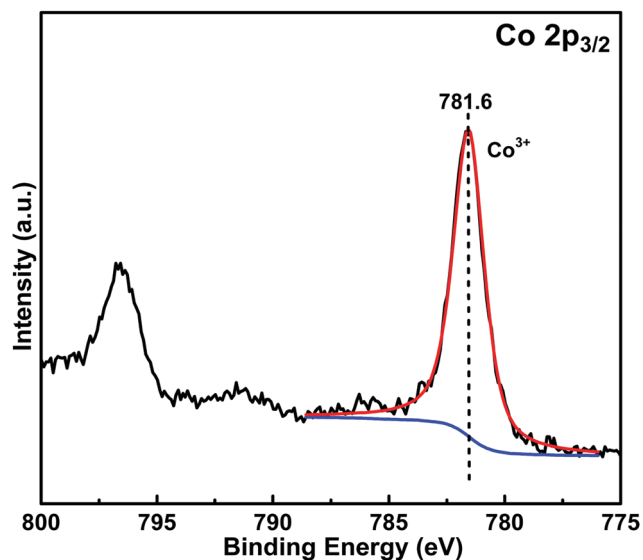


Fig. 5 XPS spectra of $[\text{Co}(\text{NH}_3)_6]\text{Cl}_3$.

of $[\text{Co}(\text{NH}_3)_6]\text{Cl}_3$. However, $[\text{Co}(\text{NH}_3)_5\text{Cl}]\text{SO}_4$ possessed a stronger acidity than $[\text{Co}(\text{NH}_3)_6]\text{Cl}_3$, which showed one peak band at 433 °C (strong acid site), indicating the enhancement of acidity by introducing SO_4^{2-} . The complexes synthesized by introducing different acid radical ions showed different reactivity in the subsequent epoxidation reaction.

3.2. Catalytic epoxidation of α -pinene

The results of different cobalt–ammonia complexes in catalyzing the epoxidation process of α -pinene are shown in Fig. 7. It could be seen that the different complexes obviously exhibited different catalytic activity. The $[\text{Co}(\text{NH}_3)_6]\text{Cl}_3$ catalyst showed the best catalytic performance with 97.4% conversion of α -pinene and

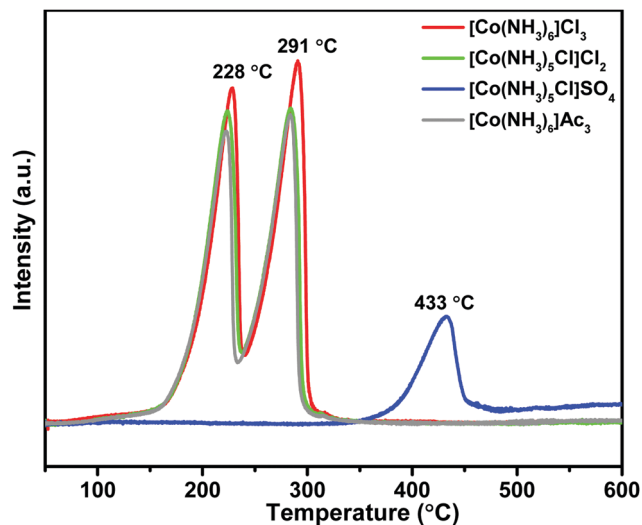


Fig. 6 NH_3 -TPD analysis results of cobalt–ammonia complexes.

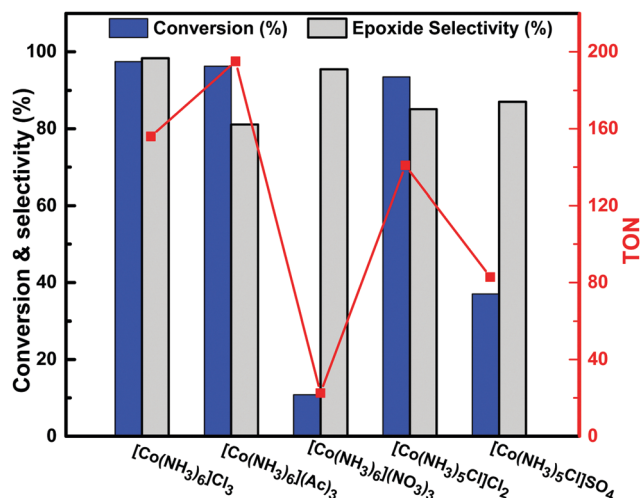


Fig. 7 The effect of different cobalt–ammonia complexes on the epoxidation of α -pinene. Conditions: catalyst, 5 mg; α -pinene, 3 mmol; solvent, DMF 10 g; initiator, CHP 0.3 mmol; temperature, 90 °C; flow rate of air, 40 mL min^{-1} ; and time, 5 h.

98.3% selectivity of epoxide. When using $[\text{Co}(\text{NH}_3)_6](\text{Ac})_3$ as the catalyst, the conversion was close to the result of using $[\text{Co}(\text{NH}_3)_6]\text{Cl}_3$ (96.2%), while its low selectivity led to the low yield of epoxide. $[\text{Co}(\text{NH}_3)_6](\text{NO}_3)_3$ only converted 10.8% of α -pinene. When using $[\text{Co}(\text{NH}_3)_5\text{Cl}]^{2+}$ class complexes with different anions, the conversion of α -pinene exhibited a significant drop from 93.5% to 37.1% after Cl_2^{2-} was replaced by SO_4^{2-} . It could be seen that different anions had a great effect on the activity of the cobalt–ammonia complexes, which resulted in a significant difference in α -pinene conversion and epoxide selectivity. Among the above catalysts, $[\text{Co}(\text{NH}_3)_6]\text{Cl}_3$ gave apparently higher conversion of α -pinene and selectivity of target product than other cobalt–ammonia complexes. The NH_3 -TPD analysis shown in Fig. 6 also supported the above conclusion. Fig. 7 also shows the TON value

of various complexes under standard conditions. Among catalysts of different cobalt-ammonia complexes, $[\text{Co}(\text{NH}_3)_6]\text{Cl}_3$, $[\text{Co}(\text{NH}_3)_6](\text{Ac})_3$ and $[\text{Co}(\text{NH}_3)_5\text{Cl}]\text{Cl}_2$ exhibited a fairly high TON value of >140 in 5 h. Other cobalt-ammonia complexes exhibited a low TON value ($[\text{Co}(\text{NH}_3)_6](\text{NO}_3)_3$, 22.5 and $[\text{Co}(\text{NH}_3)_5\text{Cl}]\text{SO}_4$, 82.8). Moreover, Table S1 (ESI[†]) compares the catalytic performance between the as-prepared $[\text{Co}(\text{NH}_3)_6]\text{Cl}_3$ and other catalysts reported; it could be seen that the $[\text{Co}(\text{NH}_3)_6]\text{Cl}_3$ catalyst in this study gave an excellent conversion for the epoxidation of α -pinene under mild reaction conditions. As shown in Fig. S4 (ESI[†]), when $[\text{Co}(\text{NH}_3)_6]\text{Cl}_3$ was used as the catalyst, the conversion of α -pinene reached 97.4%, with 98.3% selectivity of epoxide. The complexes of $[\text{Ni}(\text{NH}_3)_6]\text{Cl}_2$, $[\text{Cu}(\text{NH}_3)_6]\text{SO}_4 \cdot \text{H}_2\text{O}$ and $(\text{NH}_4)_3\text{Cl}[\text{ZnCl}_4]$ had poor catalytic activity, and α -pinene conversion could only reach 27.9%, 19.5% and 6.4%. At the same time, the related TON value was also in the descending order of $[\text{Co}(\text{NH}_3)_6]\text{Cl}_3$ (156) $>$ $[\text{Ni}(\text{NH}_3)_6]\text{Cl}_2$ (44.8) $>$ $[\text{Cu}(\text{NH}_3)_6]\text{SO}_4 \cdot \text{H}_2\text{O}$ (31.3) $>$ $(\text{NH}_4)_3\text{Cl}[\text{ZnCl}_4]$ (10.3).

As shown in Fig. 8, the effect of different reaction temperature on the epoxidation of α -pinene was explored by gradually increasing the temperature from 60 to 95 °C. It could be easily found that the reaction temperature played an important role in the epoxidation process. The conversion was only 9.1% at 60 °C but reached 92.3% at 85 °C. The yield of epoxide reached a maximum when the temperature was further increased to 90 °C, with 97.4% conversion of α -pinene and 98.3% selectivity of epoxide. However, the selectivity of epoxide declined to 86.9% as the reaction temperature was continually increased to 95 °C, with no significant improvement of conversion. This may be ascribed to the transformation from α -pinene and epoxide to by-products while increasing the temperature, further leading to a decrease in the selectivity of the target product.

As depicted in Fig. 9, the influence of reaction time on the results of epoxidation was investigated with the other reaction conditions remaining unchanged. The conversion of α -pinene

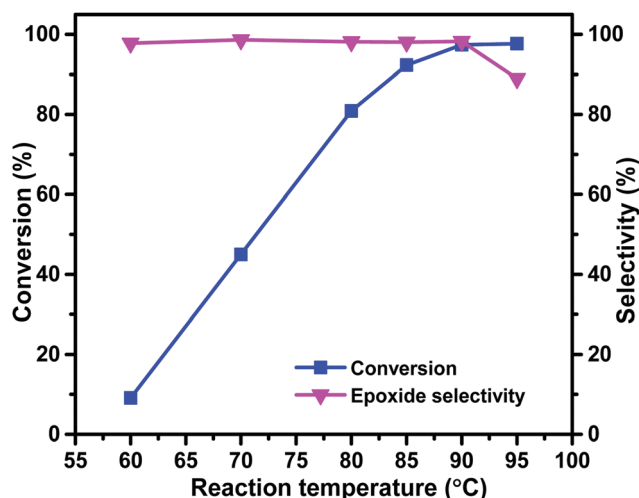


Fig. 8 The effect of reaction temperature on the epoxidation of α -pinene over $[\text{Co}(\text{NH}_3)_6]\text{Cl}_3$. Conditions: catalyst, 5 mg; α -pinene, 3 mmol; solvent, DMF 10 g; initiator, CHP 0.3 mmol; flow rate of air, 40 mL min⁻¹; and time, 5 h.

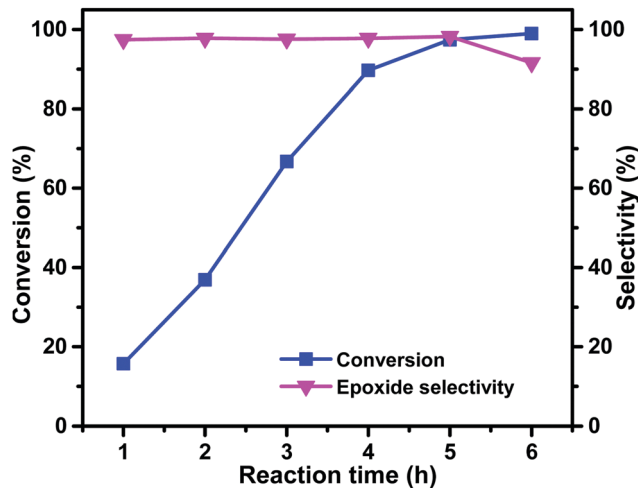


Fig. 9 The effect of reaction time on the epoxidation of α -pinene over $[\text{Co}(\text{NH}_3)_6]\text{Cl}_3$. Conditions: catalyst, 5 mg; α -pinene, 3 mmol; solvent, DMF 10 g; initiator, CHP 0.3 mmol; temperature, 90 °C; and flow rate of air, 40 mL min⁻¹.

was improved apparently at the stage of increasing the reaction time from 1 to 5 h (from 15.7% to 97.4%). However, after extending the reaction time to 6 h, the epoxide was further converted into by-products, resulting in a significant decrease in the selectivity of epoxide. Moreover, it could be seen that the conversion of α -pinene was elevated slowly at the early stage of the reaction but increased rapidly with time being extended. This may be attributed to the effect of the olefin cation radical amount, which was generated during the epoxidation process.⁵³ Less-generated radicals at the early reaction stage resulted in a slower increase rate of conversion.

As shown in Fig. 10, various initiators have been tested to promote the epoxidation of α -pinene over $[\text{Co}(\text{NH}_3)_6]\text{Cl}_3$. When

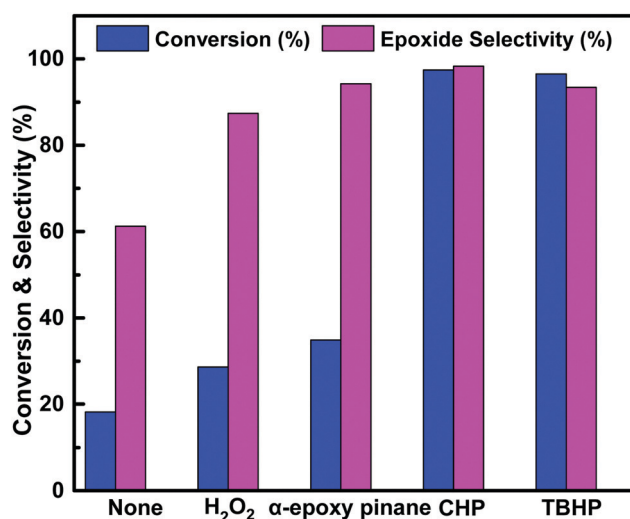


Fig. 10 The effect of different initiators on the epoxidation of α -pinene over $[\text{Co}(\text{NH}_3)_6]\text{Cl}_3$. Conditions: catalyst, 5 mg; α -pinene, 3 mmol; solvent, DMF 10 g; initiator, 0.3 mmol; temperature, 90 °C; flow rate of air, 40 mL min⁻¹; and time, 5 h.

only air was used as the oxidant without any initiators, no acceptable conversion or epoxide yield was obtained (only 18.2% conversion of α -pinene and 61.2% selectivity of epoxide). When H_2O_2 was used as the initiator, the conversion of substrate and the selectivity of target product reached 28.6% and 87.4%, respectively. It could be observed that the selectivity of epoxide was increased to 94.2% when H_2O_2 was replaced by α -epoxy pinane, whereas the conversion was still low (34.9%). When CHP or TBHP was chosen as the single initiator, the conversion was greatly increased to 97.4% and 96.5%, respectively. Moreover, the selectivity of epoxide was improved to 98.3% by using CHP, higher than that by using TBHP (93.4%). From the above results, it can be seen that CHP showed the best promoting performance for the epoxidation of α -pinene.

The effect of the amount of CHP on the reaction results is demonstrated in Fig. S5 (ESI[†]). It can be easily seen that the conversion of α -pinene and the selectivity of epoxide were both low in the absence of initiator CHP, but greatly improved (from 18.4% to 84.6% in conversion and from 60.2% to 72.1% in selectivity, respectively) by adding a small amount of CHP (0.06 mmol). When the amount of CHP was increased from 0.06 to 0.3 mmol gradually, both conversion and selectivity were elevated to 97.4% and 98.3%, respectively. However, the variation trend showed some differences when further increasing the amount of initiator to 0.4 mmol, which manifested as a continuous increase in conversion but decrease in selectivity of epoxide. From the above result, it could be seen that an appropriate amount of CHP (0.3 mmol) facilitated to maximize the yield of epoxide.

As shown in Fig. S6 (ESI[†]), the influence of different flow rates of air on the epoxidation of α -pinene over $[\text{Co}(\text{NH}_3)_6]\text{Cl}_3$ was investigated. It could be seen that only 14.7% conversion of α -pinene was obtained with no air being introduced. Then the conversion and selectivity of epoxide were gradually elevated when the flow rate of air was increased from 20 to 40 mL min^{-1} . However, a significant drop in the selectivity of epoxide was observed when the flow rate of air was further increased to 50 mL min^{-1} , accompanied by a slight increase in conversion. This may be attributed to the decomposition of epoxide, caused by excessive oxygen. Therefore, the yield of target product reached a maximum when the flow rate of air was 40 mL min^{-1} .

Fig. 11 lists the influence of different solvents on the epoxidation of α -pinene over $[\text{Co}(\text{NH}_3)_6]\text{Cl}_3$. Obviously, the reaction solvent significantly affected the epoxidation process. Due to the weak ability of dissolving oxygen, non-polar toluene gave only 7.3% conversion of α -pinene. THF seemed to be the most unsuitable one and achieved <5% conversion of α -pinene. When the polar solvents DMA and 1,4-dioxane were used, though the conversion of α -pinene was higher than when using non-polar solvents, as described above, the conversions were only 21.5% and 19.0%. The conversion reached 97.4% when strong polar DMF was selected as the reaction solvent. Owing to the strong coordination with cobalt species and O_2 , DMF played an important role in the epoxidation of α -pinene with air. Previous studies had found that $\text{Co}(\text{II})$ could effectively activate oxygen and form active intermediates with DMF, which

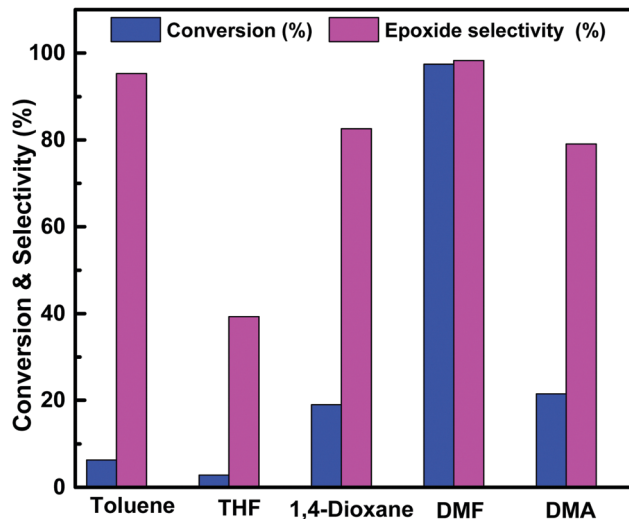


Fig. 11 The effect of solvents on the epoxidation of α -pinene over $[\text{Co}(\text{NH}_3)_6]\text{Cl}_3$. Conditions: catalyst, 5 mg; α -pinene, 3 mmol; solvent, 10 g; initiator, CHP 0.3 mmol; temperature, 90 °C; flow rate of air, 40 mL min^{-1} ; and time, 5 h.

further promoted the epoxidation reaction of α -pinene with air.^{28,36,54,55} $\text{Co}(\text{III})$ in the reaction system also played an important role in transferring oxygen.⁴⁴

The schematic illustration for the epoxidation of α -pinene is shown in Fig. S7 (ESI[†]). It could be observed that there was one main product α -pinene oxide (a) and several by-products (b–d). It is worth noting that camphorenal aldehyde (b) was the product of further isomerization of α -pinene oxide. Table 1 lists the results of α -pinene epoxidation over $[\text{Co}(\text{NH}_3)_6]\text{Cl}_3$ catalyst with different amounts of substrate. As shown in Entry 1, when the amount of α -pinene was 3 mmol, 97.4% α -pinene conversion and 98.3% epoxide selectivity were obtained. As the substrate amount increased from 3 to 6 mmol, the conversion and selectivity of epoxide still maintained around 80% and >90%, respectively. However, as the amount of substrate increased to 10 mmol, the conversion decreased rapidly to 42.3%. The reason for the drop may be the lack of active sites. The conversion reached 98.0% when 6 mmol of substrate was continuously reacted for 8 h. On the other hand, it can be seen

Table 1 The effect of substrate amount on the epoxidation of α -pinene

Entry	Substrate amount (mmol)	Time (h)	Conversion (%)	Selectivity (%)			
				a	b	c/d	Others
1	3	5	97.4	98.3	0.9	0.2/0.5	0.1
2	4	5	93.0	93.9	2.0	1.4/2.1	0.6
3	5	5	91.5	92.1	2.3	1.8/3.0	0.8
4	6	5	80.0	92.8	2.4	1.2/2.9	0.7
5	6	6	90.0	88.1	4.6	2.3/4.3	0.7
6	6	7	95.8	87.6	5.9	1.9/3.4	1.2
7	6	8	98.0	86.5	8.7	1.1/2.4	1.3
8	10	5	42.3	92.5	4.3	1.2/1.5	0.5

Conditions: catalyst, $[\text{Co}(\text{NH}_3)_6]\text{Cl}_3$ 5 mg; substrate, α -pinene; solvent, DMF 10 g; initiator, CHP 0.3 mmol; temperature, 90 °C; flow rate of air, 40 mL min^{-1} ; and time, 5 h.

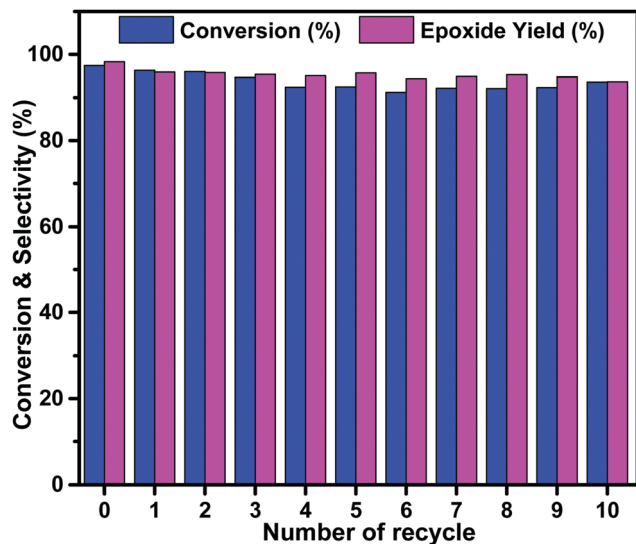


Fig. 12 Results of recyclable performance of the $[\text{Co}(\text{NH}_3)_6]\text{Cl}_3$ catalyst. Conditions: catalyst, $[\text{Co}(\text{NH}_3)_6]\text{Cl}_3$; α -pinene, 3 mmol; solvent, DMF 10 g; initiator, CHP 0.3 mmol; temperature, 90 °C; flow rate of air, 40 mL min^{-1} ; and time, 5 h.

from entries 4–7 that the selectivity of α -pinene oxide gradually declined when the reaction time was extended. Moreover, the distribution of products reflected that the proportion of camphorenaldehyde showed an obvious upward trend, which could be attributed to the further isomerization of α -pinene oxide as the reaction time extended.

The recycling experiments of the $[\text{Co}(\text{NH}_3)_6]\text{Cl}_3$ catalyst on the epoxidation of α -pinene were conducted. As shown in Fig. 12, the activity of $[\text{Co}(\text{NH}_3)_6]\text{Cl}_3$ (ten times) showed a slight decline during the initial three recycles, but was basically unchanged in the subsequent seven recycles. Negligible leaching of cobalt species from $[\text{Co}(\text{NH}_3)_6]\text{Cl}_3$ was detected by analyzing the ICP results of fresh and recycled catalysts. The XRD patterns and IR spectra of fresh and 10th recycled catalysts are compared in Fig. S8 and S9 (ESI[†]). It could be observed that the recycled catalyst had almost the same peaks as that of the fresh one in the XRD patterns or IR spectra. The favorable stability and recycling performance may be ascribed to the stable coordination environment of the Co species. Moreover, we also conducted the recycling performance of $[\text{Co}(\text{NH}_3)_5]\text{Cl}_2$. As could be seen from Fig. S10, though the catalytic activity of $[\text{Co}(\text{NH}_3)_5]\text{Cl}_2$ was lower than $[\text{Co}(\text{NH}_3)_6]\text{Cl}_3$, its conversion reached 86.4% after being recycled 5 times. From Fig. S11 (ESI[†]) it could be seen that the XRD patterns of recycled $[\text{Co}(\text{NH}_3)_5]\text{Cl}_2$ was exactly consistent with that of the fresh one, with only a little drop in the intensity of peaks. The reaction mechanism of the epoxidation reaction catalyzed by the $[\text{Co}(\text{NH}_3)_6]\text{Cl}_3$ catalyst is shown in Fig. S12 (ESI[†]). Firstly, the active intermediates formed by DMF and O_2 were adsorbed by $[\text{Co}(\text{NH}_3)_6]\text{Cl}_3$ (Step I). Then, molecular oxygen was activated by $\text{Co}(\text{III})$ to form active peroxy intermediate species (Step II). Subsequently, the α -pinene molecules interacted with peroxy intermediate species and formed cyclic intermediate species (Step III), which released epoxide molecules at last (Step IV), and then the process restarted with Step I.

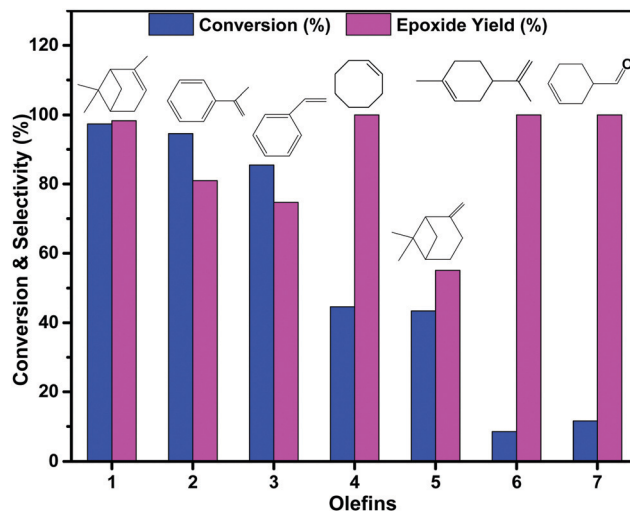


Fig. 13 The catalytic epoxidation of other bulky cycloalkenes. Conditions: catalyst, $[\text{Co}(\text{NH}_3)_6]\text{Cl}_3$ 5 mg; substrate, 3 mmol; solvent, DMF 10 g; initiator, CHP 0.3 mmol; temperature, 90 °C; flow rate of air, 40 mL min^{-1} ; and time, 5 h.

The conversion of epoxidation reaction of several cycloalkenes under the above-stated conditions is listed in Fig. 13. It can be seen that $[\text{Co}(\text{NH}_3)_6]\text{Cl}_3$ performed excellent catalytic properties on the epoxidation of some cyclic olefins. Comparatively, the conversion of alkenes declined in the order of α -pinene (97.4%) > α -methylstyrene (94.6%) > styrene (85.5%) > cyclooctene (44.6%) > β -pinene (43.4%) > 3-cyclohexene-1-carboxaldehyde (11.6%) > limonene (8.6%). However, the epoxide selectivity declined in the order of limonene (100%) = 3-cyclohexene-1-carboxaldehyde (100%) = cyclooctene (100%) > α -pinene (98.3%) > α -methylstyrene (81%) > styrene (74.7%) > β -pinene (55.1%). The epoxidation of linear terminal 1-heptene and 1-dodecene with air was negligible. The possible explanation for apparently different results on epoxidizing cyclic olefin and linear olefin was that electrophilic cycloaddition activity was weakened by the low π -electron density of linear olefin.⁵⁶

4. Conclusions

A series of cobalt–ammonia complexes with different external anions (Ac^- , NO_3^- , SO_4^{2-} , Cl^-) were prepared using a simple method and applied to catalyze the epoxidation of α -pinene to α -epoxy pinane. The experimental results showed that $[\text{Co}(\text{NH}_3)_6]\text{Cl}_3$ exhibited the best catalytic activity on the epoxidation of α -pinene. The cobalt–ammonia complex used, the catalyst amount, the reaction solvents, the reaction temperature, the reaction time and initiators exerted notable impacts on the epoxidation reaction. The considerable reaction results demonstrated that single $\text{Co}(\text{III})$ even showed better catalytic effect on epoxidation than a single $\text{Co}(\text{II})$ system. The recycling experiments indicated that $[\text{Co}(\text{NH}_3)_6]\text{Cl}_3$ was a stable and recyclable heterogeneous catalyst, which showed no significant deactivation after 10 recycles.

Conflicts of interest

There are no conflicts of interest to declare.

Acknowledgements

The authors thank the National Natural Science Foundation of China (No. 22072038, 21673069, U20A20122 and 21503074), the Hubei Student Innovation and Entrepreneurship Foundation of China (S201910512016 and S202010512082), and the Applied Basic Frontier Project of Wuhan Science and Technology Bureau (2019010701011415).

References

- O. A. Wong and Y. Shi, *Chem. Rev.*, 2008, **108**, 3958–3987.
- J. S. Jirkovsky, M. Busch, E. Ahlberg, I. Panas and P. Krtil, *J. Am. Chem. Soc.*, 2011, **133**, 5882–5892.
- U. N. Gupta, N. F. Dummer, S. Pattisson, R. L. Jenkins, D. W. Knight, D. Bethell and G. J. Hutchings, *Catal. Lett.*, 2015, **145**, 689–696.
- J. W. Brown, Q. T. Nguyen, T. Otto, N. N. Jarenwattananon, S. Glöggler and L. S. Bouchard, *Catal. Commun.*, 2015, **59**, 50–54.
- A. Ansmann, R. Kawa and M. Neuss, *US Pat.*, 7083780 B2, 2006, assigned to Cognis Deutschland.
- R. Chakrabarty, B. K. Das and J. H. Clark, *Green Chem.*, 2007, **9**, 845–848.
- A. K. Suresh, M. M. Sharma and T. Sridhar, *Ind. Eng. Chem. Res.*, 2000, **39**, 3958–3997.
- Y. Qi, Y. Luan, J. Yu, X. Peng and G. Wang, *Chem. – Eur. J.*, 2014, **20**, 1–10.
- M. Farias, M. Martinelli and D. P. Botteg, *Appl. Catal., A*, 2010, **384**, 213–219.
- K. A. Jorgensen, *Chem. Rev.*, 1989, **89**, 431–458.
- R. Mbeleck, M. L. Mohammed, K. Ambroziak, D. C. Sherrington and B. Saha, *Catal. Today*, 2015, **256**, 287–293.
- L. L. Bai, L. Yao, Y. H. Yang and J. M. Lee, *Chem. Commun.*, 2015, **51**, 4259–4262.
- E. Poli, J. M. Clacens, J. Barrault and Y. Pouilloux, *Catal. Today*, 2009, **140**, 19–22.
- N. S. Patil, R. Jha, B. S. Uphade, S. K. Bhargava and V. R. Choudhary, *Appl. Catal., A*, 2004, **275**, 87–93.
- D. S. Pinnaduwa, L. Zhou, W. W. Gao and C. M. Friend, *J. Am. Chem. Soc.*, 2007, **129**, 1872–1873.
- G. J. Hutchings, *Chem. Commun.*, 2008, 1148–1164.
- H. Tanaka, H. Nishikawa, T. Uchida and T. Katsuki, *J. Am. Chem. Soc.*, 2010, **132**, 12034–12041.
- M. Guidotti, N. Ravasio, R. Psaro, E. Gianotti, L. Marchese and S. Coluccia, *Green Chem.*, 2003, **5**, 421–424.
- J. P. Zhang, S. Nagamatsu, J. Du, C. L. Tong, H. H. Fang, D. H. Deng, X. Liu, K. Asakura and Y. Z. Yuan, *J. Catal.*, 2018, **367**, 16–26.
- M. G. Topuzovaa, S. V. Kotova and T. M. Kolev, *Appl. Catal., A*, 2005, **281**, 157–166.
- G. D. Faveri, G. Ilyashenko and M. Watkinson, *Chem. Soc. Rev.*, 2011, **40**, 1722–1760.
- X. Wang, S. Wu, Z. Li, X. Yang, H. Su, J. Hu, Q. Huo, J. Guan and Q. Kan, *Microporous Mesoporous Mater.*, 2016, **221**, 58–66.
- A. R. Yaul, G. B. Pethe and A. S. Aswar, *Russ. J. Coord. Chem.*, 2010, **36**, 254–258.
- A. E. Gerbase, J. R. Gregório, M. Martinelli, M. C. Brasil and N. F. Mendes, *J. Am. Oil. Chem. Soc.*, 2002, **79**, 179–181.
- G. S. Owens, J. Arias and M. M. Abu-Omar, *Catal. Today*, 2000, **55**, 317–363.
- S. B. Tian, Q. Fu, W. X. Chen, Q. C. Feng, Z. Chen, J. Zhang, D. S. Wang and Y. D. Li, *Nat. Commun.*, 2018, **9**, 2353–2360.
- S. Shit, D. Saha, T. G. Row and C. Rizzoli, *Inorg. Chim. Acta*, 2014, **415**, 103–110.
- B. Tang, X. H. Lu, D. Zhou, P. Tian, Z. H. Niu, J. L. Zhang, X. Chen and Q. H. Xia, *Catal. Commun.*, 2013, **31**, 42–47.
- B. Tang, X. H. Lu, D. Zhou, J. Lei, Z. H. Niu, J. Fan and Q. H. Xia, *Catal. Commun.*, 2012, **21**, 68–71.
- K. Huang, Z. L. Wang and D. F. Wu, *J. Chem. Sci.*, 2018, **130**, 62–74.
- S. Muratsugu, Z. H. Weng and M. Tada, *ACS Catal.*, 2013, **3**, 2020–2030.
- L. Canali and D. C. Sherrington, *Chem. Soc. Rev.*, 1999, **28**, 85–93.
- M. P. Fernandez-Ronco, J. Kluge and M. Mazzotti, *Cryst. Growth Des.*, 2013, **13**, 2013–2024.
- M. R. Maurya, S. Sikarwar and M. Kumar, *Catal. Commun.*, 2007, **8**, 2017–2024.
- E. Zamanifar, F. Farzaneh, J. Simpson and M. Maghami, *Inorg. Chim. Acta*, 2014, **414**, 63–70.
- X. H. Lu, J. Lei, X. L. Wei, X. T. Ma, T. J. Zhang, W. Hu, D. Zhou and Q. H. Xia, *J. Mol. Catal. A: Chem.*, 2015, **400**, 71–80.
- R. Neumann and M. Dahan, *Nature*, 1997, **388**, 353–355.
- Y. Nishiyama, Y. Nakagawa and N. Mizuno, *Angew. Chem., Int. Ed.*, 2001, **40**, 3639–3641.
- M. E. Davis, *Nature*, 2002, **417**, 813–821.
- M. Masteri-Farahani and S. Mirshekar, *Colloids Surf., A*, 2018, **538**, 387–392.
- Y. Qi, Y. Luan, J. Yu, X. Peng and G. Wang, *Chem. – Eur. J.*, 2014, **20**, 1–10.
- J. Zhao, W. Y. Wang, H. L. Tang, D. Ramella and Y. Luan, *Mol. Catal.*, 2018, **456**, 57–64.
- P. Neves, A. C. Gomes, T. R. Amarante, F. A. Paz, M. Pillinger, I. S. Gonçalves and A. A. Valente, *Microporous Mesoporous Mater.*, 2015, **202**, 106–114.
- F. A. Chavez, J. M. Rowland, M. M. Olmstead and P. K. Mascharak, *J. Am. Chem. Soc.*, 1998, **120**, 9015–9027.
- P. Buranaprasertsuk, Y. Tangsakol and W. Chavasiri, *Catal. Commun.*, 2007, **8**, 310–314.
- J. Bjerrum and J. P. McReynold, *Inorg. Synth.*, 1946, **2**, 216–221.
- D. G. Hill and A. F. Rosenberg, *J. Chem. Phys.*, 1956, **24**, 1219–1231.
- N. Tanaka and M. Nanjo, *B. Chem. Soc. Jpn.*, 1964, **37**, 1330–1332.
- K. Mech, P. Zabinski and R. Kowalik, *Electrochim. Acta*, 2012, **87**, 254–259.

- 50 G. W. Watt, *Inorg. Chem.*, 1964, **3**, 325–329.
- 51 Z. Zivkovic, *J. Therm. Anal. Calorim.*, 1994, **41**, 99–104.
- 52 B. J. Tufts, I. L. Abrahams and C. E. Caley, *J. Am. Chem. Soc.*, 1990, **112**, 5123–5136.
- 53 E. Bosch and J. K. Kochi, *J. Am. Chem. Soc.*, 1996, **118**, 1319–1329.
- 54 G. Xu, Q. H. Xia, X. H. Lu, Q. Zhang and H. J. Zhan, *J. Mol. Catal. A: Chem.*, 2007, **266**, 180–187.
- 55 P. P. Tao, X. H. Lu, H. F. Zhang, R. Jing, F. F. Huang, S. Wu, D. Zhou and Q. H. Xia, *Mol. Catal.*, 2019, **463**, 8–15.
- 56 K. H. Tong, K. Y. Wong and T. H. Chan, *Org. Lett.*, 2003, **5**, 3423–3425.